

# Single-phase cuprite thin films prepared by a one-step low-vacuum thermal oxidation technique

Wenhan Du<sup>1,2,3</sup>, Jingjing Yang<sup>1</sup> ✉, Keke Zhang<sup>3</sup>

<sup>1</sup>School of Electrical and Optoelectronic Engineering, Changzhou Institute of Technology, #666, Liaohe Road, Changzhou, Jiangsu, People's Republic of China

<sup>2</sup>Suzhou Institute of Nano-Tech and Nano-Bionic, Chinese Academy of Sciences, Suzhou, Jiangsu, People's Republic of China

<sup>3</sup>School of Materials Science and Engineering, Nanyang Technological University, Block N4.1, Nanyang Avenue, Singapore

✉ E-mail: yangjj@czu.cn

Published in *Micro & Nano Letters*; Received on 7th August 2018; Revised on 19th November 2018; Accepted on 5th December 2018

Cu<sub>2</sub>O thin film solar cells have attracted the interest of many researchers owing to their non-toxic and earth-abundant properties. High-quality pure-phase Cu<sub>2</sub>O thin films were prepared by using a simple low-vacuum thermal annealing technique. The growth temperatures of the Cu<sub>2</sub>O thin films were varied from 400 to 1000°C. X-ray diffraction (XRD) and scanning electron microscopy were used to characterise the structural and morphological changes of the thin films. The XRD results suggested that all the films were pure-phase Cu<sub>2</sub>O; thus, no second-phase CuO was observed. The detailed evolution of the surface morphology was investigated. The electron dispersion spectrum (EDS) results show that the atomic ratio of Cu and O were changed with the annealing temperature, the ratio change from around 2:1 to 1.84:1 with the turning temperature of 800°C, indicating copper vacancy formed during annealing temperature higher than 800°C. EDS results well matched the d-spacing changes of the XRD results.

**1. Introduction:** To replace fossil fuels such as coal and crude oil, the photovoltaic industry has accelerated the development of solar cells in recent years, which is beneficial for the reduction of greenhouse gas. Two types of solar cells have been introduced to the market, namely, crystalline silicon and thin film solar cells. Among the commercial thin-film solar cells, cadmium telluride (CdTe) and copper–indium–gallium–selenide (CIGS) thin film solar cells suffer from serious problems owing to the toxicity of the Cd elements used in the former and to the rarity of the In element used in the latter. To resolve these problems, researchers are investigating another type of thin film solar cell, namely, the cuprite thin film solar cell.

Owing to its non-toxic and earth-abundant property, the cuprite thin film solar cell has received attention from many researchers [1–13]. The theoretical limit of a single-junction Cu<sub>2</sub>O cell is about 20%; with the intensive investigations during the last decades. However, the experimental conversion efficiency of the cuprite thin film solar cell has passed 8% with three major improvements: first, the thermal treatment of cuprite thin films with Na ion; second, the addition of the Ga<sub>2</sub>O<sub>3</sub> buffer layer; and, third, the replacement of the ZnO thin film with the Zn<sub>1-x</sub>Ge<sub>x</sub>O thin film as the n-partner of the p–n junction [4–6]. Cuprite thin film solar cells with the highest efficiency were prepared using a thermal oxidation technique, which is far better than other techniques such as magnetron sputtering and electroplating [9–11], thermal oxidation technique is a low defect and high-quality growth method, while sputtering is a high energy growth method which caused a large number of defects in the film, the film purity prepared by electroplating was poor since the solution process of this method.

Until now, there are only a few studies on the thermal oxidation process of a copper sheet, especially the oxidation mechanism [9, 13]. Mingze *et al.* [14] reported that high vacuum (0.02 Pa) cooling is efficient to eliminate the CuO impurity and both high temperature and longtime annealing lead to preferential growth of (311) surface. Archana *et al.* [15] reported that preparation of pure phase Cu<sub>2</sub>O thin film at a reduced temperature of 300°C by intentionally controlling solely the kinetic parameter (total chamber pressure,  $P_{tot}$ ) at fixed thermodynamic condition (0.25 mTorr,  $P_{O_2}$ ).

Santos Valladares *et al.* [16] reported that the crystallisation and electrical resistivity of the formed oxides in a Cu/SiO<sub>2</sub>/Si thin film after thermal oxidation by ex-situ annealing at different temperatures up to 1000°C, the single phase Cu<sub>2</sub>O thin film was prepared at a temperature of 200°C at air condition, while the CuO phase was only prepared when the temperature was increased to higher than 200°C. Here, using X-ray diffraction (XRD) and scanning electron microscopy/electron dispersion spectrum (SEM/EDS), we used a novel low-vacuum oxidation method to investigate the thermal oxidation process of a copper sheet from 400 to 1000°C, to enhance our understanding of the formation mechanism of cuprite thin films for solar cell applications.

**2. Experiment:** Copper foil was bought from Sigma Aldrich with a thickness of 0.1 mm, and the purity was 99.95%. The foil was cut into a standard piece of 10 × 10 mm<sup>2</sup>. Before vacuum thermal annealing was carried out, the copper sheet was ultrasonic cleaned with acetone, isopropanol alcohol, and deionised water sequentially, and then blew up with high purity N<sub>2</sub> gas. Clean copper sheets were put into a quartz tube, and the vacuum pressure was pumped down to 1.0 × 10<sup>-3</sup> Torr by a mechanical pump. Then the copper sheet was heated by radiation and the temperature was monitored by a *k* type thermal couple. When the temperature reached the set value, high purity oxygen gas was introduced into the quartz tube and controlled by mass flow controller (MFC) until the chamber pressure reached 100 Torr which was monitored by a vacuum gauge. Different growth time was arranged to investigate the surface revolution. After the growth of copper oxide, the temperature of the substrate was cooled to room temperature without controlling the cooling speed, during this period the vacuum pressure was kept below 1.0 × 10<sup>-3</sup> Torr.

The crystalline structural information of the films was analysed using XRD measurement (Rigaku, Ultima IV) with Cu K $\alpha$  ( $\lambda = 1.54060 \text{ \AA}$ ). The XRD data were collected in the 2 $\theta$  range from 20° to 80° with a step size of 0.02°. The morphology information of the films was analysed by field emission SEM (Zeiss, Sigma). The element information of the films was analysed by (EDS, Oxford).

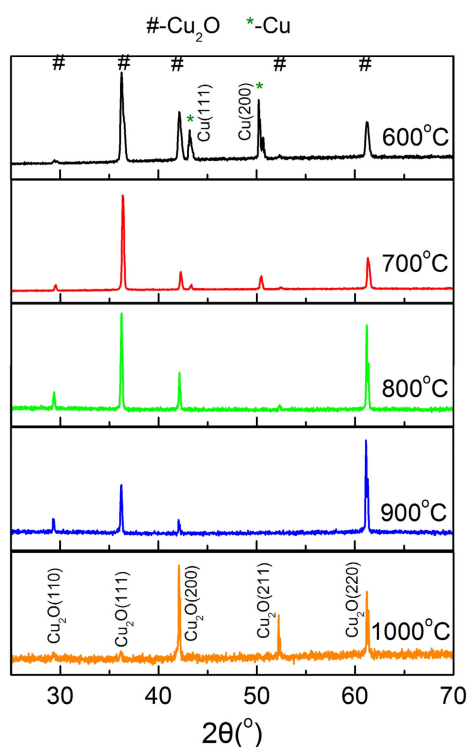


**Fig. 1** XRD results of  $\text{Cu}_2\text{O}$  thin film on copper sheet with an oxidation time of 10 min. The oxygen partial pressure was fixed at 100 Torr. The oxidation temperatures were 600, 700, 800, 900, and 1000°C

**3. Results and discussion:** Fig. 1 shows the XRD results of the  $\text{Cu}_2\text{O}$  thin films obtained by the low-vacuum oxidation method between 600 and 1000°C, the annealing time was 10 min for all the samples in this figure. From this figure, it can be seen that only pure-phase  $\text{Cu}_2\text{O}$  thin film existed as the figure shows six typical diffraction peaks, which represent the (110), (111), (200), (211), (220), and (311) planes, respectively, of the cubic  $\text{Cu}_2\text{O}$  structure. There was no other mixed oxide phase such as CuO. The oxidation temperature exerted a significant effect on the strongest peaks of  $\text{Cu}_2\text{O}$ .  $\text{Cu}_2\text{O}(111)$  was the strongest peak between 600 and 800°C, which was similar to the  $\text{Cu}_2\text{O}$  thin film prepared by a sputtering technique [17, 18]. When the temperature was increased to 1000°C, the strongest peak shifted to  $\text{Cu}_2\text{O}(200)$ . The strongest diffraction peak was  $\text{Cu}_2\text{O}(220)$  at an annealing temperature of 900°C.

The crystalline parameter changes of the four different lattice planes, namely,  $\text{Cu}_2\text{O}(110)$ ,  $\text{Cu}_2\text{O}(111)$ ,  $\text{Cu}_2\text{O}(200)$ , and  $\text{Cu}_2\text{O}(220)$ , were investigated further. The variations in the lattice constant (d-spacing), grain size, and full width at half maximum (FWHM) at different oxidation temperatures are shown in Fig. 2. The grain size increased with the increase in annealing temperature. The maximum grain size was nearly 130 nm calculated by the Scherrer equation. The FWHM decreased with the increase in annealing temperature. The minimum FWHM value was  $<0.1^\circ$ . These two parameters change with temperature variation can be explained by the improvement in the crystalline quality as the temperature increased. However, the changes in the other parameter, i.e. the lattice constant (d-spacing), were quite different from those of the grain size and the FWHM. The value of the lattice constant of these four planes was obviously lowest near the oxidation temperature of 600–800°C, and it increased when the oxidation temperature increased to 1000°C or decreased to 400°C, indicating that something different happened at the temperature range of 600–800°C.

To determine the reason for the lattice constant bowing effect with temperature and to understand the oxidation mechanism

further, we explored the surface morphology changes at different oxidation temperatures. Figs. 3 and 4 show the SEM images of  $\text{Cu}_2\text{O}$  at different oxidation temperatures. The grain size increased significantly with the increase in oxidation temperature from 600

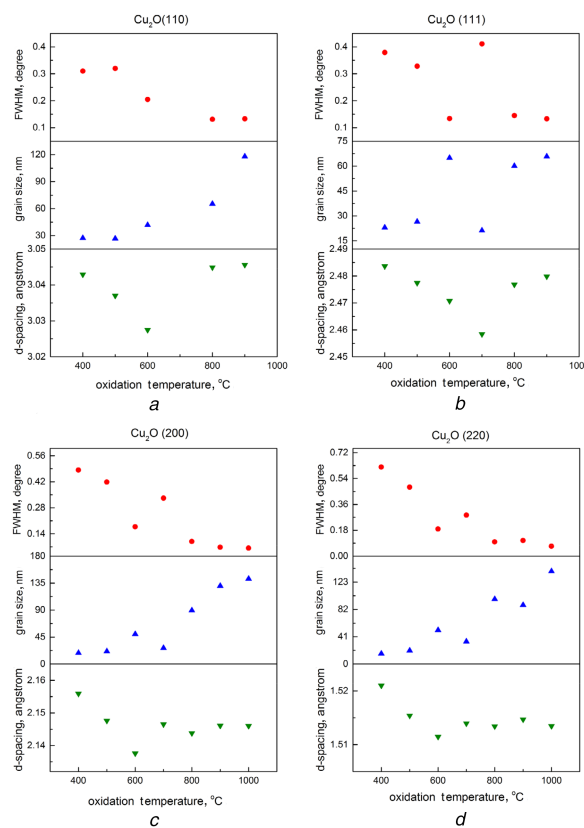


**Fig. 2** XRD parameter of different crystalline orientation changes with the oxidation temperature. The oxygen partial pressure was fixed at 100 Torr. Four different lattice planes are shown as  
a  $\text{Cu}_2\text{O}(110)$   
b  $\text{Cu}_2\text{O}(111)$   
c  $\text{Cu}_2\text{O}(200)$   
d  $\text{Cu}_2\text{O}(220)$

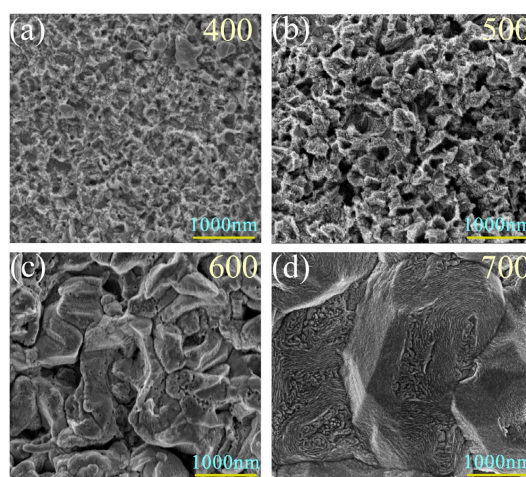


**Fig. 3** SEM results of  $\text{Cu}_2\text{O}$  thin films with low annealing temperatures. All the samples were prepared at an oxygen partial pressure of 100 Torr and the oxidation time was 10 min. The oxidation temperatures were  
a 400°C  
b 500°C  
c 600°C  
d 700°C

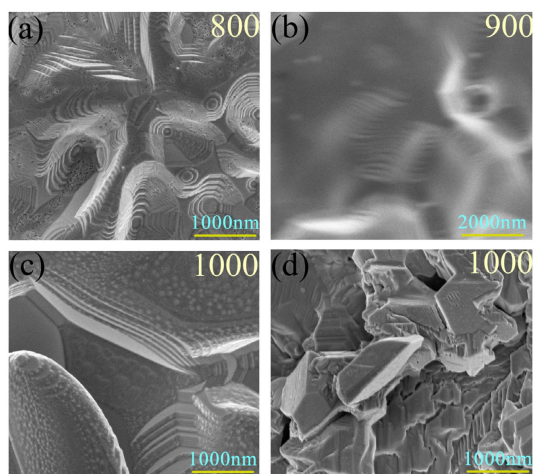


**Fig. 4** SEM results of  $\text{Cu}_2\text{O}$  thin films with high annealing temperatures. The difference between Figs. 4c and d was oxidation time, and the oxidation temperature was the same at  $1000^\circ\text{C}$ . All the samples were prepared at an oxygen partial pressure of 100 Torr and the oxidation time was 10 min, except Fig. 4d with the annealing time of 30 min. The oxidation temperatures were  
 a  $800^\circ\text{C}$   
 b  $900^\circ\text{C}$   
 c and d  $1000^\circ\text{C}$

to  $700^\circ\text{C}$ , and a terrace appeared in the SEM image when the oxidation temperature was increased to  $800^\circ\text{C}$ . These big changes in the SEM images support the lattice constant changes at the temperature range of  $600\text{--}800^\circ\text{C}$ . Small grains appeared in the large grain terrace as shown in Fig. 4c at an oxidation temperature of  $1000^\circ\text{C}$  and an oxidation time of 10 min, whereas large grains broke into small grains when the oxidation time increased from 10 to 30 min, as shown in Fig. 4d. The case in Fig. 4b was special because, at an oxidation temperature of  $900^\circ\text{C}$ , the conductivity was poor, and therefore, no clear SEM image could be obtained. All the SEM images features matched well with the XRD results.

Furthermore, we measured the detailed changes of Cu/O atomic ratio from EDS. The EDS results of different annealing temperature samples in Table 1 showed that at a relatively low annealing temperature such as lower than  $600^\circ\text{C}$  the Cu/O atomic ratio was approximately 2:1, when the annealing was temperature higher than  $700^\circ\text{C}$ , the Cu/O atomic ratio will be reduced to around 1.8:1, indicating that there will exist a copper vacancy in the cuprite thin film. The Cu/O atomic ratio changes in EDS explained well d-spacing changes in the XRD results, as copper vacancy easily formed when the annealing temperature was higher than  $600^\circ\text{C}$  at a low vacuum condition, which is supported by the large quantity of small holes in Fig. 3(c) and 3(d), when the annealing temperature was higher than  $800^\circ\text{C}$ , which also proved by the SEM images in Fig. 4, as large quantity terrace formed during atomic movement, and the copper atom will easily

**Table 1** Cu/O atomic ratio obtained from EDS data at room temperature

Annealing temperature, $^\circ\text{C}$	Cu atomic percent	O atomic percent	Cu:O atomic ratio
400	66.9	33.1	2.02
500	65.9	34.1	1.93
600	66.0	34.0	1.94
700	65.0	35.0	1.86
800	64.5	35.5	1.82
900	64.8	35.2	1.84
1000	64.8	35.2	1.84

move into the vacuum chamber from the terrace and leave a copper vacancy in the cuprite thin film. Since the cooling speed was fast (about  $200^\circ\text{C}/\text{min}$  between  $600$  and  $1000^\circ\text{C}$ ), and copper vacancy in the sample was kept at room temperature. The different contents of copper vacancy contribute to the d-spacing changes in the cuprite thin film prepared at a different temperature.

**4. Conclusion:** High-quality pure-phase  $\text{Cu}_2\text{O}$  thin films were prepared using a low-vacuum thermal annealing technique. Moreover, the growth temperature was controlled between  $400$  and  $1000^\circ\text{C}$ . The XRD results showed that pure-phase cuprite thin films could be prepared without a second-phase  $\text{CuO}$ . An abnormal phenomenon was observed after a detailed analysis of the lattice constant changes in the temperature range of  $600\text{--}800^\circ\text{C}$ , because of the terrace formation in the SEM images. Detailed EDS results show that the Cu/O atomic ratio was about 2:1 at lower annealing temperatures, while it will change to about 1.8:1 at annealing temperature higher than  $700^\circ\text{C}$ , thus forming copper vacancy in cuprite thin film and reducing the d-spacing value of  $\text{Cu}_2\text{O}(200)$  and  $\text{Cu}_2\text{O}(220)$  grains, well matched the d-spacing changes in XRD results.

**5. Acknowledgments:** This work was supported by the Project of Cooperative Innovation Fund of Jiangsu Province with grant no. BY2018150; Changzhou Sci & Tech Program with grant no. CZ20180015, startup Foundation of Changzhou Institute of Technology with grant no. YN1710.

## 6 References

- Pan J., Yang C., Gao Y.: 'Investigations of cuprous oxide and cupric oxide thin films by controlling the deposition atmosphere in the reactive sputtering method', *Sens. Mater.*, 2016, **28**, (7), pp. 817–824
- Wang Y., Ghanbaja J., Soldera F., *ET AL.*: 'Tuning the structure and preferred orientation in reactively sputtered copper oxide thin films', *Appl. Surf. Sci.*, 2015, **335**, pp. 85–91
- Yantara N., Pham T.T.T., Boix P.P., *ET AL.*: 'Modulating light propagation in ZnO- $\text{Cu}_2\text{O}$ -inverse opal solar cell', *Phys. Chem. Chem. Phys.*, 2015, **17**, pp. 21694–21701
- Minami T., Nishi Y., Miyata T.: 'Efficiency enhancement using a Zn1-x GexO thin film as an n-type window layer in  $\text{Cu}_2\text{O}$ -based heterojunction solar cells', *Appl. Phys. Express*, 2016, **9**, p. 052301
- Minami T., Nishi Y., Miyata T.: 'Heterojunction solar cell with 6% efficiency based on an n-type aluminum-gallium-oxide thin film and p-type sodium-doped  $\text{Cu}_2\text{O}$  sheet', *Appl. Phys. Express*, 2015, **8**, p. 022301
- Minami T., Nishi Y., Miyata T.: 'High-Efficiency  $\text{Cu}_2\text{O}$ -based heterojunction solar cells fabricated using a  $\text{Ga}_2\text{O}_3$  thin film as N-type layer', *Appl. Phys. Express*, 2013, **6**, p. 044101
- Necmi S., Tülay S., Seyda H., *ET AL.*: 'Annealing effect on the properties of copper oxide thin films prepared by chemical deposition', *Semicond. Sci. Technol.*, 2005, **20**, pp. 398–401
- Jatinder K., Ole B., Rachmat A.W., *ET AL.*: 'All-oxide solar cells based on electrodeposited  $\text{Cu}_2\text{O}$  absorber and atomic layer deposited ZnMgO on precious-metal-free electrode', *Sol. Energy Mater. Sol. Cells*, 2017, **161**, pp. 449–459
- Yuki N., Toshihiro M., Tadatsugu M.: 'Electrochemically deposited  $\text{Cu}_2\text{O}$  thin films on thermally oxidized  $\text{Cu}_2\text{O}$  sheets for solar cell applications', *Sol. Energy Mater. Sol. Cells*, 2016, **155**, pp. 405–410
- Tadatsuga M., Toshihiro M., Yuki N.: 'Relationship between the electrical properties of the n-oxide and p- $\text{Cu}_2\text{O}$  layers and the photo-voltaic properties of  $\text{Cu}_2\text{O}$ -based heterojunction solar cells', *Sol. Energy Mater. Sol. Cells*, 2016, **147**, pp. 85–93
- Ooi P.K., Ng S.S., Abdullah M.J., *ET AL.*: 'Effects of oxygen percentage on the growth of copper oxide thin films by reactive radio frequency sputtering', *Mater. Chem. Phys.*, 2013, **140**, pp. 243–248
- Jayatissa A.H., Guo K., Jayasuriya A.C.: 'Fabrication of cuprous and cupric oxide thin films by heat treatment', *Appl. Surf. Sci.*, 2009, **255**, pp. 9474–9479
- Figueiredo V., Elangovana E.: 'Effect of post-annealing on the properties of copper oxide thin films obtained from the oxidation of

- evaporated metallic copper', *Appl. Surf. Sci.*, 2008, **254**, pp. 3949–3954
- [14] Mingze S., Zhimin L., Chuanxi Z., *ET AL.*: 'Preparation of high quality Cu<sub>2</sub>O crystal and its optp-electronic properties', *Mater. Lett.*, 2016, **170**, pp. 80–84
- [15] Archana S., John D.P., Ryan P.O., *ET AL.*: 'Non equilibrium deposition of phase pure Cu<sub>2</sub>O thin films at reduced temperature', *APL Mater.*, 2014, **2**, p. 022105
- [16] Santos Valladares L., Salinas D.H., Dominguez A.B., *ET AL.*: 'Crystallization and electrical resistivity of Cu<sub>2</sub>O and CuO obtained by thermal oxidation of Cu thin films on SiO<sub>2</sub>/Si substrate', *Thin Solid Films*, 2012, **520**, pp. 6368–6374
- [17] Du W.H., Yang J.J., Xiong C., *ET AL.*: 'Preferential orientation growth of ITO thin film on quartz substrate with ZnO buffer layer by magnetron sputtering technique', *Int. J. Mod. Phys. B*, 2017, **31**, (16–19), p. 1744065
- [18] Du W.H., Yang J.J., Zhao Y., *ET AL.*: 'Preparation of ZnS by magnetron sputtering and its buffer effect on the preferential orientation growth of ITO thin film', *Micro Nano Lett.*, 2018, **13**, (4), pp. 506–508